ANALYSIS OF FLOC STRUCTURE BASED ON THE EXTENDED BRINKMAN MODEL

LECH GMACHOWSKI, MASASHI IWATA, TAKEHITO ADACHI AND TOSHIRO MURASE

Department of Chemical Engineering, Nagoya University, Nagoya 464-01

Key Words: Solid Liquid Separation, Flocculation, Brinkman Model, Floc Density Function, Floc Fractal Dimension, Permeability, Polystyrene

The extended Brinkman model for flocculated dispersion is presented. This model can describe fluid flow relative to a swarm of flocs over a wide concentration range. The theoretical floc density function is derived by combining the model with the permeability data in a concentrated region where individual flocs contact each other. For flocculated polystyrenes consisting of non-porous, impermeable, and spherical particles of submicron size, the density, the aggregation number, and the projected area diameter of a floc were determined by the sedimentation method, the drying method, and the photographic method, respectively. The permeability data in dilute and concentrated regions were obtained by the sedimentation test and the constant-rate expression method, respectively. Agreement between the theoretical floc density function and experimental floc characteristics was satisfactory. The floc morphology was strongly reflected in the permeability characteristic in a concentrated region. It was found that the overall solidosity when complete floc breakage occurs is approximately equal to that of the loosest packing structure of a sphere bed.

Introduction

Flocculation is an essential stage in solid-liquid separation processes when solid particles to be separated are too small to make the processes effective. Particles are then caused to aggregate to form a larger unit. The structure of formed flocs depends on the interaction between particles,[2] as well as on the mechanism of the collisions between the aggregating objects. The latter factor involves mainly the aggregation sequence. Two simple limiting cases are the single-particle addition model and the aggregation model of two identical clusters. Computer simulations performed by Sutherland and Geodarz-Nia show that a floc produced by the former model is denser than one formed by the latter when both flocs contain the same number of primary particles.[18] It is evident that in reality there are collisions between clusters of different aggregation numbers. The structure of the formed floc is related to the fractal dimension of a floc.[16]

The fractal dimension is a measure of how particles fill the space of an aggregate. It can be easily found by plotting, on a long-log scale, the mass of the aggregate as a function of its characteristic length, e.g. the radius. The slope of the plot is a fractal dimension, F, of the aggregate. For an object of uniform internal structure the density is independent of its size, and a plot of the logarithmic mass vs. the logarithmic radius should give a straight line with a slope of 3.

In general, the resulting plots for aggregates give straight lines, but their slopes are less than 3. Using the fractal dimension F, there is thus the following proportionality between the aggregation number N_f of a floc and its radius R_f[5]:

$$N_f \sim R_f^F \tag{1}$$

Since the aggregation number of a floc obeys the following proportionality

$$N_f \sim (1-\varepsilon_f) R_f^3 \tag{2}$$

the floc solidosity (packing fraction) $(1-\varepsilon_f)$ depends on the floc radius

$$(1-\varepsilon_f) \sim R_f^{F-3} \tag{3}$$

The last proportionality expresses the floc density function, experimentally found by Tambo and Watanabe.[19]

In the previous paper,[12] it is shown that Eq. (3) can be derived from the extended Brinkman model[1,8] which describes fluid flow relative to a swarm of flocs. The average characteristics of flocculated Korean kaolin were well estimated by the model.

In this paper, we examine the model with respect to individual floc characteristics, i.e. the effective density and aggregation number of a floc. In this study we used polystyrene flocs which consist of mono-sized primary particles. The state of complete floc breakage under system thickening will be also dis-

* Received January 11, 1990. Correspondence concerning this article should be addressed to T. Murase. L. Gmachowski is at Institute of Physical Chemistry, Polish Academy of Sciences, 01-224 Warsaw, Poland.

cussed.

1. Theory

The presence of voids in a floc brings about internal permeability. During the movement of such a floc relative to the surrounding liquid, the liquid flows not only around but also through the floc. When flocs are approximately spherical, the liquid flow relative to a swarm of the flocs can be described by the model created by Brinkman[1] and corrected by Gmachowski.[8] The final result of the model can be presented as an interdependence of three dimensionless parameters[8,12]:

$$f(\lambda R_f, PR_f, \delta^3)=0 \tag{4}$$

where $1/\lambda^2$ is the whole-medium permeability, $1/P^2$ is the floc permeability, and δ^3 is the volume fraction of flocs, i.e.

$$\delta^3=(1-\varepsilon)/(1-\varepsilon_f) \tag{5}$$

where $(1-\varepsilon)$ is the overall solidosity of flocculated suspensions.

This model has experimental support reported by Gmachowski.[6,10] In the works cited, the empirical plots of λ vs. $(1-\varepsilon)$ were well fitted by Eqs. (4) and (5) under the condition that the floc characteristics R_f, P, and $(1-\varepsilon_f)$ were constant.

For flocculated dispersions of higher concentration where flocs contact each other, it is impossible to fit the experimental data to the theoretical curve for any constant floc characteristics. This is because concentrated flocculated dispersions obey the following power law, experimentally shown by Egolf and McCabe,[4] Grace,[7,13] and us.[12,15]

$$\lambda=const_1(1-\varepsilon)^n \tag{6}$$

The variability of floc characteristics along this line can be analyzed as follows.[11] From Eq. (6) one can derive the following equations.

$$d\ln\lambda/d\ln(1-\varepsilon)=n \tag{7}$$

$$d^2\ln\lambda/d\{\ln(1-\varepsilon)\}^2=0 \tag{8}$$

If floc characteristics R_f and $(1-\varepsilon_f)$ are fixed,

$$d\ln\lambda R_f/d\ln\delta^3=d\ln\lambda/d\ln(1-\varepsilon) \tag{9}$$

$$d^2\ln\lambda R_f/d(\ln\delta^3)^2=d^2\ln\lambda/d\{\ln(1-\varepsilon)\}^2 \tag{10}$$

From Eqs. (7)$\sim$(10) one obtains

$$d\ln\lambda R_f/d\ln\delta^3=n \tag{11}$$

$$d^2\ln\lambda R_f/d(\ln\delta^3)^2=0 \tag{12}$$

The flocculated dispersion that satisfies both Eqs. (4) and (6) consequently appears as the inflection point on a $\ln\lambda R_f-\ln\delta^3$ curve calculated from Eq. (4) for a given PR_f. The constancy of PR_f for fixed floc characteristics R_f and $(1-\varepsilon_f)$ is evident, since P is a unique function of $(1-\varepsilon_f)$ for a given solid-liquid system. The values of PR_f, λR_f and δ^3 at the inflection point are unique functions of the power n of Eq. (6) and are marked as

$$PR_f=const_2 \tag{13}$$

$$\lambda R_f=const_3 \tag{14}$$

$$\delta^3=const_4 \tag{15}$$

These values can be calculated from Eqs. (4) and (6) and correlated with the n-value.

$$\left.\begin{aligned} const_2&=6.80n^{1.70} \quad \text{for} \quad 0.8<n<3\\ const_2&=5.46n^{1.90} \quad \text{for} \quad 3<n<8 \end{aligned}\right\} \tag{16}$$

$$\left.\begin{aligned} const_3&=3.85n^{1.47} \quad \text{for} \quad 0.8<n<3\\ const_3&=2.15n^{2.00} \quad \text{for} \quad 3<n<8 \end{aligned}\right\} \tag{17}$$

$$const_4=0.539n^{0.228} \quad \text{for} \quad 0.8<n<8 \tag{18}$$

Although Eqs. (9) and (10) are valid for any floc characteristics, R_f and $(1-\varepsilon_f)$ must be chosen to fulfil the coordinates of the inflection point. For a point $(\lambda, (1-\varepsilon))$ of the line described by Eq. (6), they should be

$$R_f=const_3/\lambda \tag{19}$$

$$1-\varepsilon_f=(1-\varepsilon)/const_4 \tag{20}$$

The above discussion of floc characteristics was concerned with one point of the line described by Eq. (6). This procedure can be repeated for other mixture concentrations to obtain the variability of floc characteristics with system thickening. As a result, the floc radius diminishes with the system solidosity according to the following equation, derived from Eqs. (6) and (19).

$$R_f=(const_3/const_1)(1-\varepsilon)^{-n} \tag{21}$$

Equation (21) is a mathematical description of the phenomenon of floc breakage under a thickening process of a solid-liquid system. It is also possible to calculate the solidosity of a floc using Eqs. (5), (15) and (21).

$$1-\varepsilon_f=\{(const_3/const_1)^{1/n}/const_4\}R_f^{-1/n} \tag{22}$$

In the above theoretical discussion we obtain a relation between the floc solidosity and the radius, and we can hence call Eq. (22) the theoretical floc density function. It should be valid up to the state of complete floc breakage, i.e. the state where no floc exists and the solid-liquid mixture contains only primary particles. The form of the theoretical floc density function (Eq. (22)) is similar to that described by Eq. (3). Hence it is assumed that there is an analogy between floc formation and breakage. The floc

formation process is illustrated in **Fig. 1**, where for simplicity the cluster-cluster aggregation model is assumed. The size of the finally formed flocs may be adjusted according to flocculant dosage and mixing strength. In the previous work,[12] it is shown that the size of Korean kaolin floc depends on the dosage of flocculant, whereas the n-values are almost the same for each suspension.

If the characteristics R_f, P and $(1-\varepsilon_f)$ of flocs are fixed, Eq. (4) can be simplified as

$$\lambda = f(1-\varepsilon) \qquad \text{for constant } R_f,\ P \text{ and } (1-\varepsilon_f) \tag{23}$$

Eq. (23) is schematically shown by the broken lines in **Fig. 2** on a log-log plot. It is evident that the larger the flocs, the lower situated the curve. At higher concentrations where flocs contact each other, the floc characteristics are no longer constant and the curves transit into a solid straight line of slope n (the thickening line), which is a graphical representation of Eq. (6). All points on the solid line correspond to the inflection point of the model curve ($\ln \lambda R_f$ vs. $\ln \delta^3$ curve for constant PR_f) given by Eq. (4).

Any further thickening after flocs contact each other brings about floc breakage, the reverse of floc formation. In this state the flocs form a network-like structure caused by a rapid increase in floc-floc contact number. A reflocculation phenomenon occurs by the same forces which previously brought about aggregation. This is possible because a given particle interacts not only with the remaining particles in the floc but also with those belonging to other flocs. The reflocculation consists of disaggregation and secondary aggregation into smaller units, and for that reason it may be called floc breakage. The current floc size in the breakage region can be calculated by Eq. (21) (see Fig. 6). The thickening line in Fig. 2 is limited by the point corresponding to the complete breakage of flocs.

Such a picture of system thickening and breakage of aggregates of different starting size has been confirmed experimentally for aqueous suspensions of Korean kaolin[12] and polymer solutions.[8,9]

In the state of complete breakage of aggregate, a given solid-liquid system contains only primary particles. According to the above theory, the primary particles should also have the characteristics which fulfill Eqs. (13) and (16). However, it is rather a very special case, since the most usual situation in practice is such that the primary particles are nonporous and impermeable. Nevertheless, Eq. (6) holds, which suggests that real systems have the same mechanism of floc breakage. We accordingly assume that the real flocculated system is equivalent to a hypothetical system consisting of ideal primary particles, for which the model is fully consistent. Based on this assumption,

Fig. 1. Schematic picture of flocculation process (Cluster-cluster aggregation model)

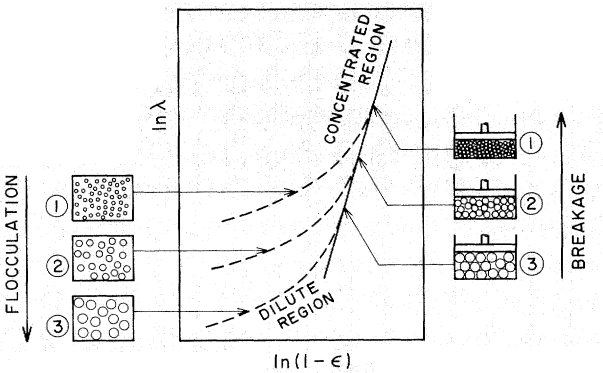

Fig. 2. Relation between floc formation and breakage

$R_f \neq R_p$ at the state of complete breakage of flocs, where R_p is the radius of the primary particle, and only the aggregation number

$$N_f = R_f^3(1-\varepsilon_f)/R_p^3 \tag{24}$$

should be unity, so that

$$R_{cb}^3(1-\varepsilon_f) = R_p^3 \tag{25}$$

Here R_{cb} denotes the radius of a hypothetical primary particle when complete floc breakage occurs. Using Eqs. (22) and (24) one obtains

$$N_f = \{(const_3/const_1)^{1/n}/(const_4 R_p^3)\} R_f^{3-1/n} \tag{26}$$

where the exponent $(3-1/n)$ is the theoretical expression of floc fractal dimension F (see Eq. (1)).

In the following, the floc size and solidosity, experimentally determined for individual flocs, will be compared with the theoretical floc density function (Eq. (22)), calculated from the Brinkman model using the slope n of the thickening line (Eq. (6)). This is similar to the situation verified for polymer solutions, where the theoretical and empirical polymer coil density functions are identical.[17]

2. Materials

The experimental materials used in this study are polystyrene in the form of monosize spheres synthesized by a soap-free polymerization method proposed by Matsumoto and Ochi.[14] An electron micrograph of polystyrene particles is presented in **Fig. 3**.

Three populations of polystyrene particles with volume mean diameters of 0.656 μm, 0.667 μm and 0.737 μm, respectively, were used. The flocculated suspensions labeled 1, 2, 3 and 4 in **Fig. 4** were prepared as follows. A 200-ml flocculant solution was added to a colloidal dispersion of equal volume in a 500-ml

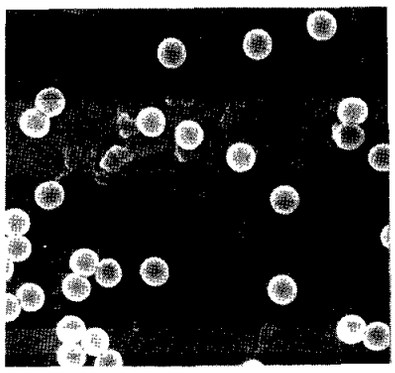

Fig. 3. Electron micrograph of polystyrene particles

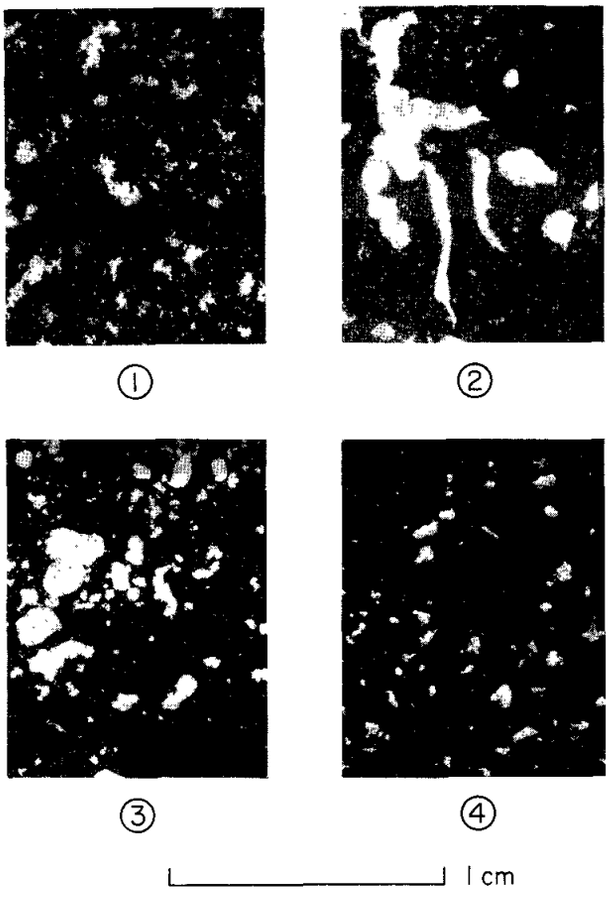

Fig. 4. Morphology of flocs

beaker. The suspension was mixed using a stirrer of paddle size 20 × 50 mm at 100 r.p.m. for 5 min. Aluminum sulfate and cationic polymers (polyacrylic acid ester, Kurita Water Industries Ltd. CP 659 and CP 648) were used as flocculants. Based on Kurita's manual, CP 659 and 648 are classified as low- and medium-charge density cationic flocculants respectively. Suspension 1 was prepared using aluminum sulfate; 2-CP 659; 3 and 4-CP. 648. Suspension 4 resulted from stirring suspension 3 at 300 r.p.m. for 2 min. The floc size distributions of these suspensions

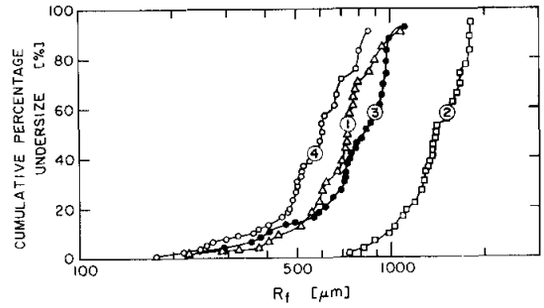

Fig. 5. Floc size (projected area radius) distributions determined by photographic method. Cumulative percentage (% in volume)

are shown in **Fig. 5**.

3. Experimental Procedures

3.1 Determination of system permeability

The permeability characteristics were determined by the sedimentation method with respect to dilute systems; i.e. λ was determined from the initial settling velocity v_0 of suspensions.

$$\lambda=\sqrt{\frac{(1-\varepsilon)(\rho_s-\rho)g}{\mu v_0}} \tag{27}$$

where ρ_s and ρ are the density of solid and liquid, respectively; g, the gravitational accelaration; and μ, the viscosity of liquid. The true density of polystyrene is obtained from gravimetric measurements, giving ρ_s of 1050 kg/m^3. For concentrated systems, the constant-rate expression method was used,[15] based on the phenomenon of fluid flow through a stationary, nearly homogeneous floc bed of controlled thickness.

3.2 Determination of individual floc characteristics

The floc density was measured by the sedimentation method and the drying method. In the sedimentation method, several flocs were introduced into a settling tank of 170 × 10 mm cross section. The time required to settle 1 − 5 cm distance was measured for one of these flocs. When this observed floc reached a certain point in the tank, it was photographed. The effective floc density ρ_e[19] was calculated from the equation

$$\rho_e=\rho_f-\rho=3\rho u^2 C_D/(4gD_f) \tag{28}$$

where ρ_f is the floc density; u, the setting velocity of the floc; and D_f, the projected area diameter of the floc. The drag coefficient C_D in Eq. (28) was calculated from Concha-Almendra's equation.[3]

$$C_D=0.28(1+9.06/Re^{0.5})^2 \tag{29}$$

In the drying test, a photograph of an individual floc on a Petri dish was taken first. The floc was then dried using a thermobalance, which can detect a 10 μg change of weight.

4. Results and Discussion

Figures 6, 7 and **8** show the variation of the whole

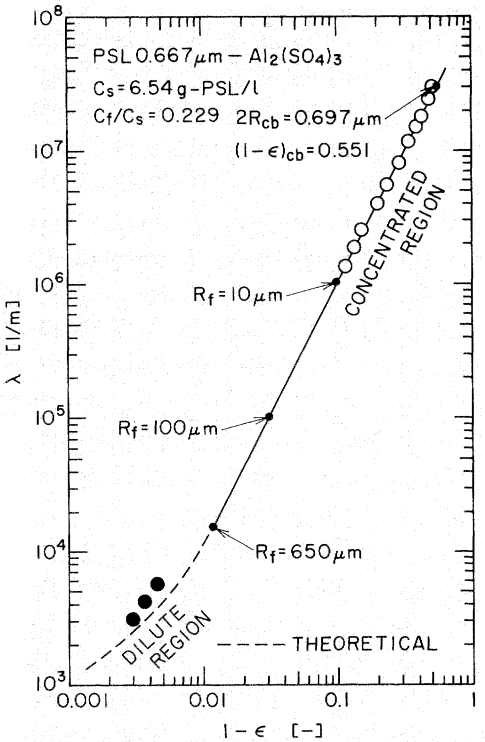

Fig. 6. Permeability characteristics of flocculated mixture (inorganic flocculant)

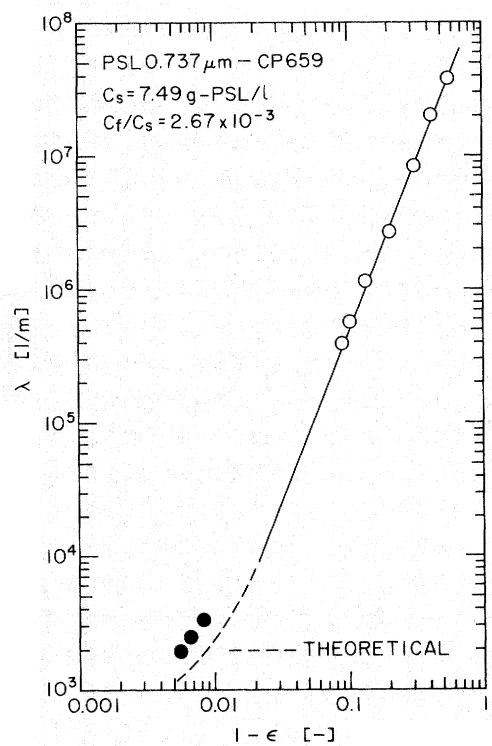

Fig. 7. Permeability characteristics of flocculated mixture (cationic polymer flocculant of low charge density)

medium permeability with the overall solidosity. Plots on $\ln\lambda$ vs. $\ln(1-\varepsilon)$ in the concentrated region can be represented by Eq. (6) (solid lines in the figures). The values of $const_1$ and n for these suspensions appear

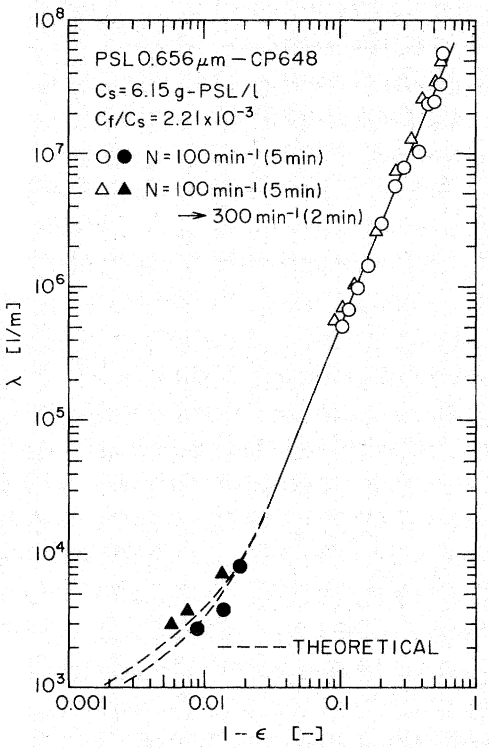

Fig. 8. Permeability characteristics of flocculated mixture (cationic polymer flocculant of medium charge density)

in **Table 1**. In the dilute region, since flocs do not contact each other, the floc characteristics are constant. The average floc radius $R_{f\cdot av}$ in this region can be defined as[12]

$$R_{f\cdot av}=\left(\frac{\Sigma n_i R_{fi}^3}{\Sigma n_i R_{fi}^{3-1/n}}\right)^n \tag{30}$$

where n_i is the number of flocs of radius R_{fi}. Broken lines in the figures are the theoretical values in the dilute region calculated as follows. Using $R_{f\cdot av}$ and n-values and Eqs. (13), (16), (17), (18) and (22), one can determine P and $(1-\varepsilon_f)$ at the transition point from the dilute to the concentrated region. Remembering that they are constant in the whole dilute region, one obtains the $\lambda-(1-\varepsilon)$ relation using Eq. (23). Agreement between theoretical and experimental values is satisfactory.

The change of floc radius R_f with system thickening is shown in Fig. 6. In the figure, $(1-\varepsilon)_{cb}$ is the value of overall solidosity when complete floc breakage occurs. R_{cb} is calculated from Eq. (26), i.e. R_f-value for $N_f=1$. $(1-\varepsilon)_{cb}$ is obtained from Eq. (21), where $R_f=R_{cb}$. The values of R_{cb} and $(1-\varepsilon)_{cb}$ are summarized in Table 1. It can be seen from the table that the values of R_{cb} are very close to those of R_p, i.e. the hypothetical primary particle with radius R_{cb} can be recognized as consisting of one primary particle and the least amount of surrounding liquid. It is also interesting that the values of $(1-\varepsilon)_{cb}$ are close to the solidosity of the loosest packing structure of sphere

Table 1. Floc characteristics

Suspension	R_p [μm]	$const_1$ [m^{-1}]	n [—]	$R_{f\cdot av}$ [μm] (dilute region)	R_{cb} [μm]	$(1-\varepsilon)_{cb}$ [—]
1 (Fig. 6)	0.334	9.54×10^7	1.96	650	0.348	0.551
2 (Fig. 7)	0.369	1.61×10^8	2.53	1360	0.388	0.570
3 (Fig. 8)	0.328	1.58×10^8	2.53	702	0.339	0.606
4 (Fig. 8)	0.328	1.58×10^8	2.53	544	0.339	0.606

bed ($1-\varepsilon=0.524$).

The purpose of the permeability determination was to obtain the values of $const_1$ and n in the concentrated region which are supposed to be connected with the floc fractal dimension. **Figures 9** and **10** show the variation of the effective floc density ρ_e with floc diameter D_f. The empirical points are obtained from settling data and Eq. (28), while theoretical lines are calculated from the following equation.

$$\rho_e=(\rho_s-\rho)(1-\varepsilon_f)$$
$$=\{(\rho_s-\rho)(const_3/const_1)^{1/n}/const_4\}R_f^{-1/n} \quad (31)$$

In Eq. (31), $const_1$ and n are known from the experimentally determined form of the thickening line, and $const_3$ and $const_4$ are calculated by Eqs. (17) and (18), respectively. In **Figs. 11** and **12**, the aggregation number N_f of a floc from a drying experiment is compared with the theoretical value from Eq. (26). It can be seen from Figs. 9~12 that, despite some scattering of experimental points, they are pretty close to the theoretical lines, i.e. the floc morphology is closely related to the permeability characteristics of the concentrated dispersions.

The scattering of data is caused by both the stochastic character of the flocculation process and experimental error. The final flocs of a given aggregation number may result from a different sequence of collisions and hence their sizes and densities may differ to some extent. Therefore the floc size and density for a given aggregation number seem to be random variables with some probability distributions. Only the mean values should correspond to the theoretical lines. Among many possible sources of error, that connected with the diameter determination of a floc seems to be the most influential. The shape of flocs is very irregular and hence the projected area of a floc is strongly dependent on how it is situated in relation to the observer. These deviations and errors may cancel one another, if the sizes are averaged. The resulting average radius corresponds well with the permeability data in a dilute region as shown in Figs. 6, 7 and 8.

Conclusions

The theoretical floc density function can be derived by combining the extended Brinkman model with the permeability data in a concentrated region. The experimental data for flocculated polystyrene, i.e. the density and aggregation number of an individual floc and permeability data in a dilute region, support this theory. The mechanism of floc breakage in a thickening process is thus closely related to the floc structure resulting from a given flocculation process; the floc morphology is closely reflected in the permeability characteristics in the concentrated

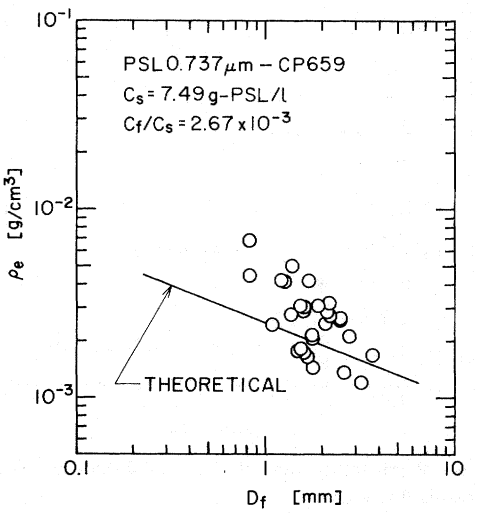

Fig. 9. Change of effective floc density ρ_e with floc diameter D_f

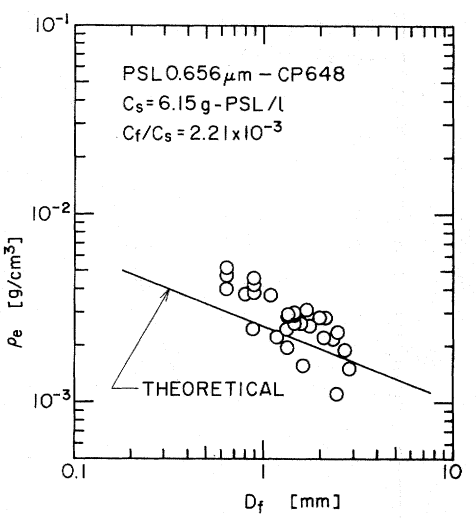

Fig. 10. Change of effective floc density ρ_e with floc diameter D_f

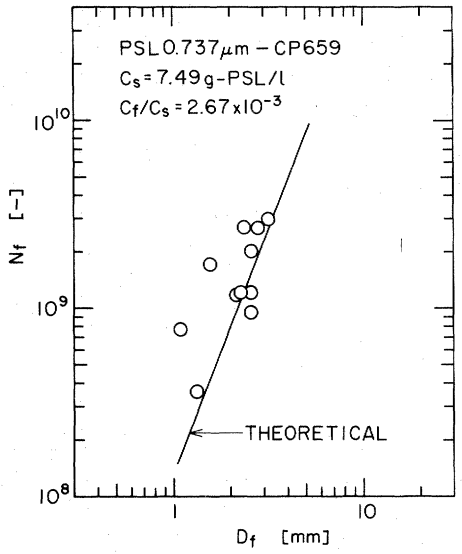

Fig. 11. Change of aggregation number N_f with floc diameter D_f

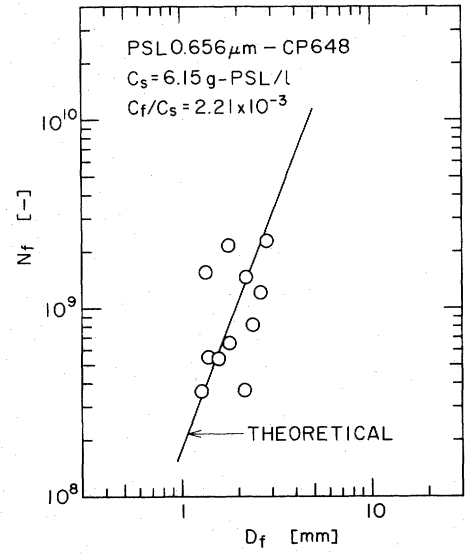

Fig. 12. Change of aggregation number N_f with floc diameter D_f

region.

Nomenclature

C_f	=	flocculant concentration in post-flocculation mixture	[kg/m^3]
C_s	=	solid concentration in post-flocculation mixture	[kg/m^3]
$const_1$	=	constant defined by Eq. (6)	[m^{-1}]
$const_2$, $const_3$ and $const_4$	=	PR_f, λR_f and δ^3 values respectively which satisfy both Eqs. (4) and (6)	[—]
D_f	=	floc diameter	[m]
F	=	fractal dimension of a floc	[—]
N_f	=	aggregation number of a floc, i.e. number of primary particles in a floc	[—]
n	=	exponent defined by Eq. (6)	[—]
P	=	reciprocal square root of floc permeability	[m^{-1}]
R_{cb}	=	radius of a hypothetical primary particle	[m]
Re	=	Reynolds number, defined by $Re = D_f \rho u/\mu$	[—]
R_f	=	floc radius	[m]
R_p	=	radius of a primary particle	[m]
δ^3	=	volume fraction of flocs	[—]
$1-\varepsilon$	=	overall solidosity of a solid-liquid system	[—]
$(1-\varepsilon)_{cb}$	=	overall solidosity when complete floc breakage occurs	[—]
$1-\varepsilon_f$	=	solidosity of a floc	[—]
λ	=	reciprocal square root of overall permeability of a solid-liquid system	[m^{-1}]
ρ	=	liquid density	[kg/m^3]
ρ_e	=	effective floc density	[kg/m^3]
ρ_s	=	solid density	[kg/m^3]

Literature Cited

1) Brinkman, H. C.: *Appl. Sci. Res.*, **A1**, 81 (1948).
2) Cohen R. D.: *AIChE J.*, **33**, 1571 (1987).
3) Concha, F. and E. R. Almendra: *Int. J. Min. Proc.*, **5**, 349, (1979).
4) Egolf, C. B. and W. L. McCabe: *Trans. AIChE*, **33**, 620 (1937).
5) Feder, J., T. Jossang and E. Rosenqvist: *Phys. Rev. Lett.*, **53**, 1403 (1984).
6) Gmachowski, L.: Proc. 2nd National Meeting "Filtration and Separation," 65, Warsaw (1984).
7) Gmachowski, L.: Proc. World Congress III of Chemical Engineering, **Vol. 3**, 150, Tokyo (1986).
8) Gmachowski, L.: *Polym. J.*, **18**, 783 (1986).
9) Gmachowski, L.: *Polym. J.*, **18**, 791 (1986).
10) Gmachowski, L.: presented at 9th CHISA Congress, 353rd Event of European Federation of Chemical Engineering, Prague (1987).
11) Gmachowski, L.: *Polym. J.*, **20**, 1073 (1988).
12) Gmachowski, L., T. Murase, M. Iwata, T. Adachi and M. Shirato: *J. Chem. Eng. Japan*, **22**, 60 (1989).
13) Grace, H. P.: *Chem. Eng. Prog.*, **49**, 303 (1953).
14) Matsumoto, T. and A. Ochi: *Kobunshi Kogaku*, **22**, 481 (1965).
15) Murase, T., M. Iwata, T. Adachi, L. Gmachowski and M. Shirato: *J. Chem. Eng. Japan*, **22**, 378 (1989).
16) Rácz, Z.: in "Fractals in Physics," edited by L. Pietronero and E. Tosatti, Elsevier Science Publishers B. V., 309 (1986).
17) Roots, J. and B. Nyström: *Polymer*, **20**, 148 (1979).
18) Sutherland, D. N. and I. Goodartz-Nia: *Chem. Eng. Sci.*, **26**, 2071 (1971).
19) Tambo, N. and Y. Watanabe: *Water Res.*, **13**, 409 (1979).

(Presented at the 54th Annual Meeting of The Society of Chemical Engineers, Japan, at Kobe, April, 1989).